



Contact angle and rivulet width hysteresis on metallic surfaces. Part I: With heated surface

Andrzej Gajewski *

Białystok Technical University, Faculty of Civil Engineering and Environmental Engineering, Department of Heat Engineering, Wiejska 45E, 15-351 Białystok, Poland

ARTICLE INFO

Article history:

Received 20 May 2008

Available online 23 July 2008

Keywords:

Contact angle

Rivulet

Hysteresis

Liquid–gas interfaces

Solid–liquid interfaces

Laser methods

ABSTRACT

The paper presents the experimental set up and the results of investigations into the contact angle and width of rivulets on aluminium, brass and copper. The measurements were taken for the increase, decrease and subsequent increase of the flow rate. As a result the hysteresis of the contact angle and rivulet width was observed. It was noticed that aluminium and brass lose their hydrophobic properties under flow conditions. They became hydrophilic materials. Copper has the worst wetting properties. It was observed that the wetting properties of sessile drops and rivulets can differ significantly. It is supposed that the more electrons there are on the last shell, the more hydrophilic a metal is under water rivulet flow.

© 2008 Elsevier Ltd. All rights reserved.

1. Introduction

Many processes realized in power, petrochemical, food-processing industries and environmental engineering or conservation use thin layers of liquid for the transfer of mass or heat. A thin layer of liquid that covers the whole surface of a solid is called a film. Hence, the contact angle equals zero. If another thin layer of liquid covers only a part of a solid surface it will be a rivulet and then the contact angle is greater than zero.

Hobler, who researched the stability of thin liquid films, distinguished three different minimum wetting rates for which the film does not break down [1]:

- $\Gamma_{\min 0}$ – during the increase of mass flow rate on the previously dry surface;
- $\Gamma_{\min 1}$ – as above but on the initially wetted surface,
- $\Gamma_{\min 2}$ – when the mass flow rate was decreased.

In each experiment the following inequality was observed:

$$\Gamma_{\min 0} > \Gamma_{\min 1} > \Gamma_{\min 2}. \quad (1)$$

It is the experimental proof of the existence of wetting hysteresis under flow conditions.

The experimental investigation into rivulets conducted by: Towell and Rothfeld [3], Semiczek-Szulc and Mikielwicz [4], Hirasawa and Hauptmann [5] as well as the results presented in [10]

prove that the contact angle is not only a function of the material properties of a three-phase system (a solid phase, a liquid, a gas or a vapour) but is also dependent on hydrodynamic phenomena. Marumur's investigations [7] and [8] lead to the conclusion that the thickness and composition of a surface-active subfilm influence the value of the static contact angle. It appears, from the above discussion, that the contact angle is affected by many factors, so measurement of the contact angle for a liquid in flow must be very complex.

Taking into account the complex nature of the wetting phenomenon, the author decided to measure the contact angle and width of rivulets on previously dry and wetted surfaces for increasing and decreasing mass flow rates. The experiments are divided into two parts. The first part was conducted with the temperature of the surface slightly higher than that of the surrounding air, so the plates were dried and the water microfilm evaporated. Rivulet flow along a dry surface occurs, e.g., in steam generators, where water evaporates from a surface. The second stage was conducted with the temperature of the surface cooler than the surrounding air and water, so that the water subfilm was present throughout the experiment, which is typical of steam condensers, for example.

2. Experiment

The approach of Langmuir and Schaefer [2], as developed by the author, was used as a measurement method. The principle of the contact angle measurement and the measurement uncertainty are described in detail in paper [11]. The temperature of the plates was about 2 K above the temperature of the surrounding air. This

* Tel.: +48 85 7 46 96 90; fax: +48 85 7 46 95 59.

E-mail address: gajewski@pb.edu.pl

Nomenclature

g gravitational acceleration,
 \dot{m} mass flow rate,
 M dimensionless mass flow rate,
 w width of the rivulet,
 W dimensionless rivulet width.

Greek symbols

Γ mass flow rate per unit width,
 θ contact angle,

μ dynamic viscosity,
 ρ density of liquid,
 σ surface tension.

Subscript

min minimum.

ensured that the plates were dry because the water evaporated from their surface.

2.1. The experimental set up

The apparatus for the investigation of gravitationally driven rivulets is shown in Fig. 1. The rivulet was photographed with a CCD camera (5) and its width was measured on a monitor screen (6) with professional computer software. A laser (3) with a graduated screen (4) was used to measure the contact angle of the rivulets. A pump (19) was used to force a flow. The upper tank (21) provided a constant flow, which was adjusted by a rotameter (17a). The plate (2) was maintained at the required

temperature by heating the water in the ultrathermostat (7) and pumping it through the double spiral channel made in the heated plate (8). If the temperature of the plate had to be lower than the surrounding air, then the water was cooled in an ice bank (9) placed before the ultrathermostat (7). With some modifications the apparatus can be used to investigate sessile drops.

2.2. Results

Because hysteresis is one of the properties of the wetting phenomena, the investigations were conducted for increasing, decreasing and again increasing mass flow rate.

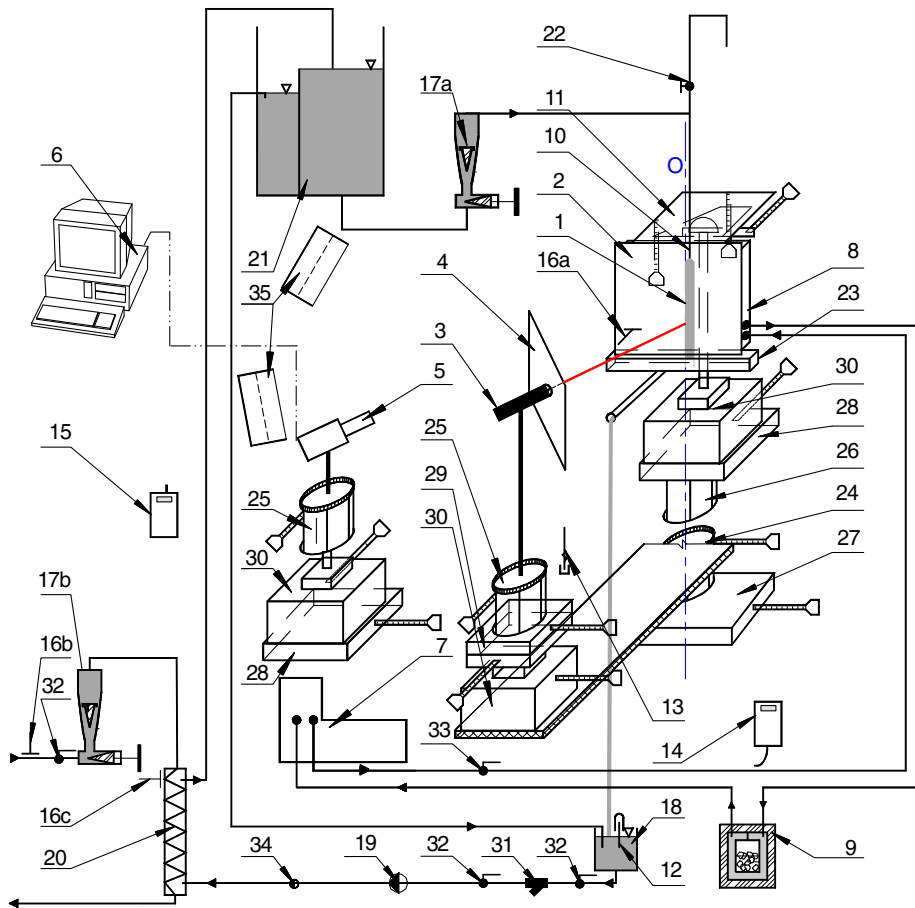


Fig. 1. The experimental apparatus: 1 – rivulet, 2 – test plate, 3 – laser, 4 – graduated screen, 5 – CCD camera, 6 – personal computer, 7 – ultrathermostat, 8 – heated plate, 9 – ice bank, 10 – needle, 11 – table regulated in three directions, 12 – thermometer, 13 – relative humidity and temperature probes, 14 – thermo-hygrometer, 15 – barometer, 16 – resistance thermometer probes, 17 – rotameters, 18 – gravity feed tank, 19 – pump, 20 – water cooler, 21 – upper tank, 22 – air valve, 23 – drainpipe, 24,25 – elements of precise rotation, 26 – rotator, 27,28 – tables of precise horizontal movement, 29 – table of precise movement in two horizontal directions, 30 – elements of vertical movement, 31 – filter, 32,33 – valves, 34 – return valve, 35 – photographic lamps.

The experimental findings are presented in the dimensionless form. The dimensionless width and mass flow rate are derived in paper [10]:

$$W = \frac{w}{\sqrt{\frac{\sigma}{\rho g}}}, \quad (2)$$

$$M = \frac{\dot{m}}{\sqrt{\frac{\sigma^2}{\mu g}}}. \quad (3)$$

Plates made of aluminium, brass and copper were immersed in distilled water for 24 h as soon as they had been sanded down. During that time, water was adsorbed and the first adsorbed layer was homogenous. This is very important for the experiments because the big differences between the contact angle values on both rivulet edges and abrupt adsorption were avoided. According to the BET theory, in the first adsorbed layer the energy of bonds is comparable to energy of chemical bonds. The energy of subsequent layers is of the same order as the energy of condensation. The BET theory has been proved by earlier experiments [12].

The present experiments were done several years after the plates had been prepared. As a consequence they were carried out in conditions similar to the technical ones but some chemical reactions may have occurred and the surfaces of the plates may have lost their homogeneity.

The width of the rivulet was measured by means of photographs with the benchmark of a linear dimension, see in Fig. 3.

2.3. Observations and discussion

The results are divided into three sections: for the increase of flow rate, its decrease and again for another increase. Two forms of reflected laser beam were observed on the screen: an elliptical triangle or a broken line, see Fig. 2. For the smallest flow rates the image on the screen had the shape of an elliptical triangle, while a broken line was observed for the bigger flow rates. The first point at which the image changed to a broken line is labelled with the letter “B” on the graph. Similarly, when the flow rate was decreasing, the point at which the broken line changed to an elliptical triangle is denoted by the letter “E”. If a change of image was observed only on one side of the rivulet, the graphs of both edges are labelled.

If the image has the shape of a motionless elliptical triangle, the author supposes that the flow is laminar. This results from the laws



Fig. 3. The unstable and asymmetrical rivulet flow on the copper plate with $M = 0.003825$, i.e., the third plotted point in Fig. 12. The picture shows the laser beam star and the black circle as the benchmark of a linear dimension.

of optical geometry: if a beam is reflected from a cylindrical surface at any angle, its image will be an ellipse. If the angle of the reflection equals $\pi/2$, the ellipse will be a circle, but it is impossible for this to be the case at every point on the surface of the rivulet because it is curved and the radius of the laser beam is not equal to zero. If the elliptical triangle oscillates around a point in the horizontal direction, the flow can change to a wavy one, as the motion of the image results from the changing rivulet width. When the crest of wave crosses the incident beam the elliptical triangle on screen moves forward. When the trough is shifting through the beam the triangle moves back. The broken line on the screen may result from the horizontal component of the motion which is perpendicular to the main stream. Such a flow can be turbulent. No expansion of rivulet was noted when the elliptical triangle was observed.

The measurements of rivulets are a lot more difficult than the experiments with sessile drops. This is caused by worse hydrophilic behaviour on the previously dry surface under flow conditions. In the case of water, brass has the best wetting properties for $M < 0.00685$, however aluminium is the best for the higher flow rates. Copper has the worst wetting properties. The observed situation differs from the static conditions where brass is more hydrophobic than aluminium but copper is the best wetted material. According to the definition, the hydrophobic state occurs only when the contact angle is higher than $\pi/2$. This situation is very difficult to observe and even more complex to measure because in this case the equilibrium state of the rivulet is unstable. Any slight disturbance moves the body to another state of equilibrium. In the experiment, the flow itself is a source of disturbance. The unstable behaviour under flow conditions manifests itself in the movement or curve of the rivulet across the plate (cf. Figs. 3 and 6) or the lack of symmetry shown in Figs. 4 and 8 as well as the split of the main stream, see Fig. 5. Therefore, when the contact angle rises above $\pi/2$, the rivulet changes its path: it widens or moves across the plate, the path may be straight or curved, and the shape may or may not be symmetrical.

Water has the most curved path on copper, which makes the measurements on copper the most difficult. It is a completely disparate situation from that observed for sessile drops, where copper is the most hydrophilic substance, which makes the experiment the easiest. Therefore, the hydrophobic or hydrophilic properties under flow conditions should be investigated separately from the static conditions.

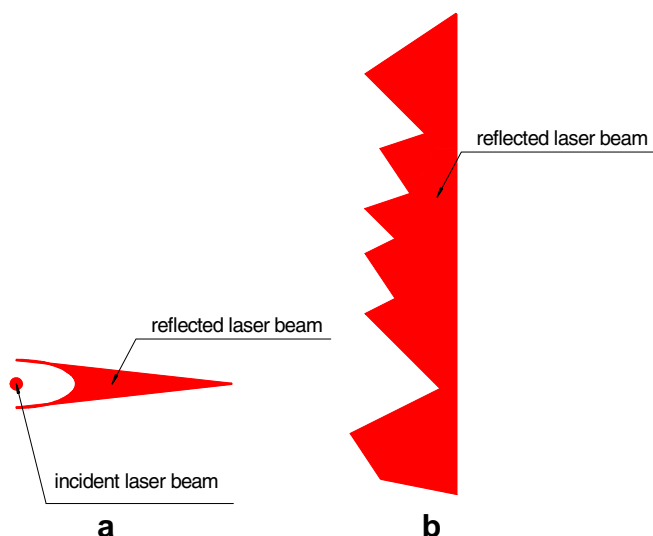


Fig. 2. The shapes of reflected laser beam on the screen: (a) an elliptical triangle, (b) a broken line.



Fig. 4. The asymmetrical rivulet flow on the copper plate with $M = 0.008197$, i.e., the last plotted point in Fig. 12.

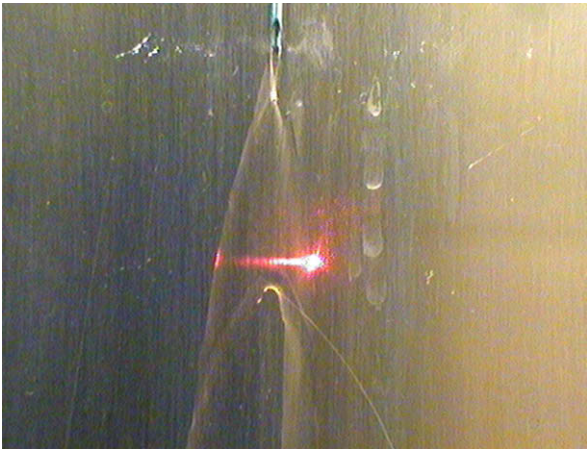


Fig. 5. The rivulet split into two on the copper plate.

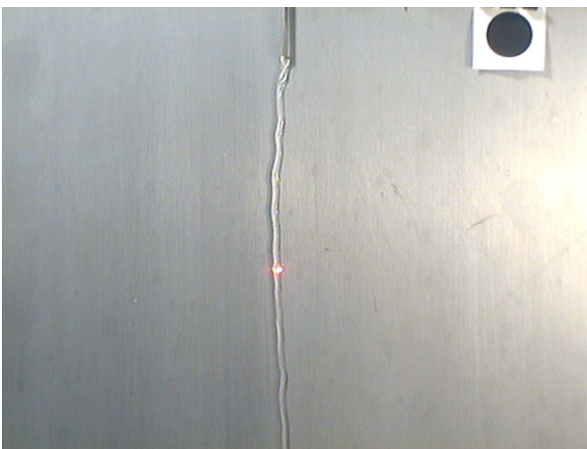


Fig. 6. The photograph of the rivulet on aluminium with $M = 0.002706$, i.e., the first plotted point in Fig. 18.

2.3.1. The increase of flow rate

At the beginning of the experiments it is observed that rivulet widths on the copper and aluminium plates have nearly the same values, but on the brass plate the rivulet is wider (cf. Figs. 12, 15 and 18). This is a different observation from that for sessile drops,

where the diameter of very small drops is a function of neither material nor roughness, but for bigger drops the widest diameter is observed on copper. For the bigger flow rates, the rivulet on brass spreads more easily than on aluminium or copper, but finally the widest rivulet is on aluminium. Copper is the least wetted

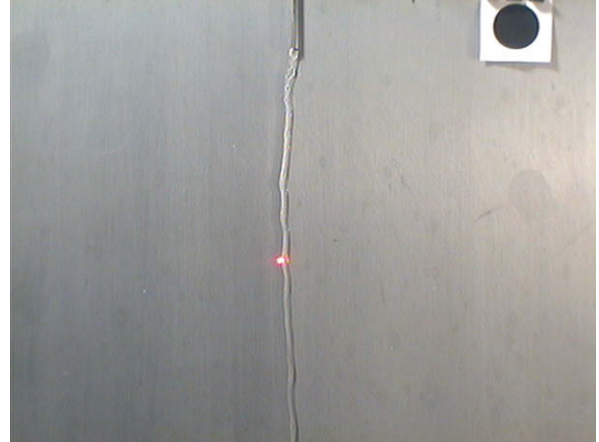


Fig. 7. The photograph of the rivulet on aluminium with $M = 0.003248$, i.e., the second plotted point in Fig. 18.

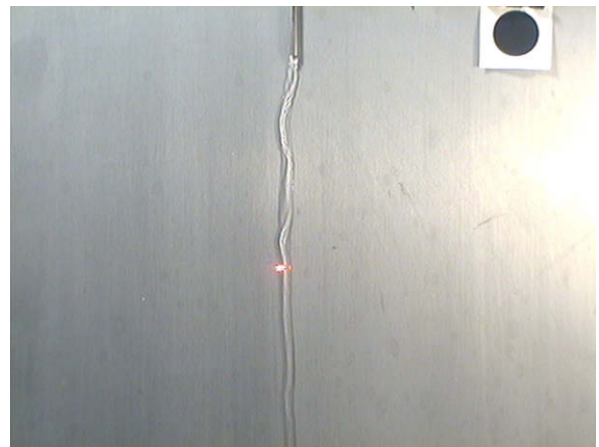


Fig. 8. The asymmetrical rivulet flow on the aluminium plate with $M = 0.00733$, i.e., the fourth plotted point in Fig. 18.

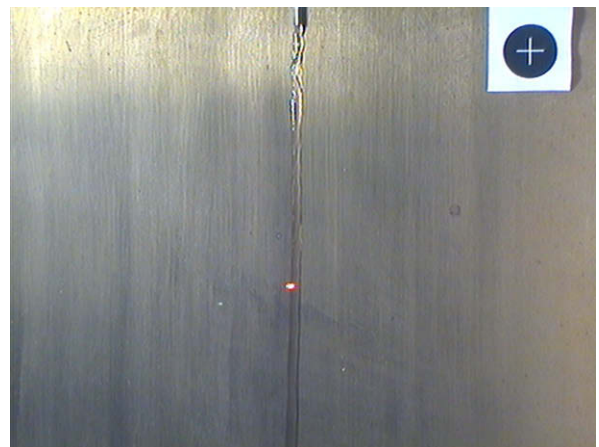


Fig. 9. The symmetrical rivulet flow on the brass plate with $M = 0.002936$, i.e., the second plotted point in Fig. 15.



Fig. 10. The asymmetrical rivulet flow on the brass plate with $M = 0.004893$, i.e., the sixth plotted point in Fig. 15.

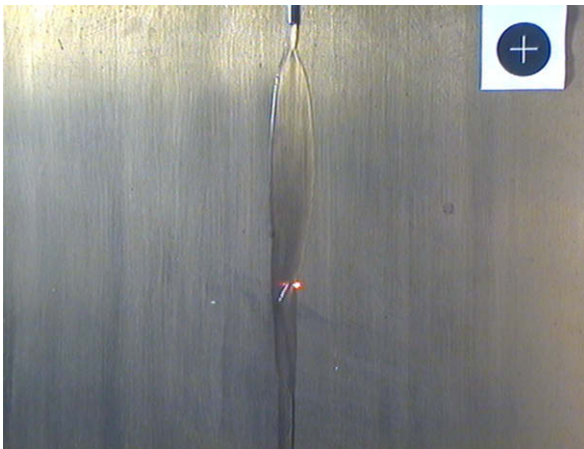


Fig. 11. The asymmetrical rivulet flow on the brass plate with $M = 0.005383$, i.e., the seventh plotted point in Fig. 15.

material, in contrast to the static conditions, in which copper is the most hydrophilic of the presented metals.

The smallest differences between the contact angle values on both sides of rivulets are observed on the brass plate, followed by copper and aluminium. In the case of aluminium the disparities are very significant.

The process of rivulet expansion on copper cannot be systematized. These experiments are the most difficult of the investigated metals. When the rivulet widens, its shape and flow path can change separately or simultaneously. Big changes of contact angle are observed between the two consecutive points and big differences between the contact angle values on the two edges.

The rivulet widening on brass can be divided into two stages. In the first stage (for $M < 0.00294$) the rivulet has a constant width and the contact angle increases. In the second phase, for higher mass flow rates, the rivulet widens but the contact angle decreases and increases by turns. The constant rivulet width between the 6th and 7th plotted points results from the asymmetrical flow (cf. Figs. 10 and 11). This asymmetry is not a property of the flow on brass but it might be caused by a local heterogeneity of the plate.

The experiments on aluminium are more difficult than on brass, but they are both much easier than on copper. The main problem is the grey colour of the aluminium surface. In consequence the dry and wetted areas are very difficult to distinguish. In addition, the rivulet on aluminium loses its symmetry at a lower flow rate than on brass (cf. Figs. 6 and 9). The worse wetting properties of water on aluminium can be confirmed by the irregular and asymmetrical flow (i.e., presented in Figs. 6–8) and the high values of the contact angle (see in Fig. 18). Moreover, very significant differences in the contact angles between the two sides of the rivulet may be a symptom of heterogeneity of the aluminium surface. Despite the fact that in the first stage (for $M < 0.003248$) the rivulet width is constant, the mean contact angle decreases. It may seem either a contradiction or even a failure of the mass balance. But it was caused by the significant asymmetry of the rivulet (cf. Figs. 6 and 7). In the second phase (for $0.003248 < M < 0.006495$) the rivulet widens but the contact angle decreases, increases and then decreases again. Significant changes in the value of the contact angle are observed, and big differences between its magnitude on the edges. Therefore, the water flow down the aluminium surface is very asymmetrical.

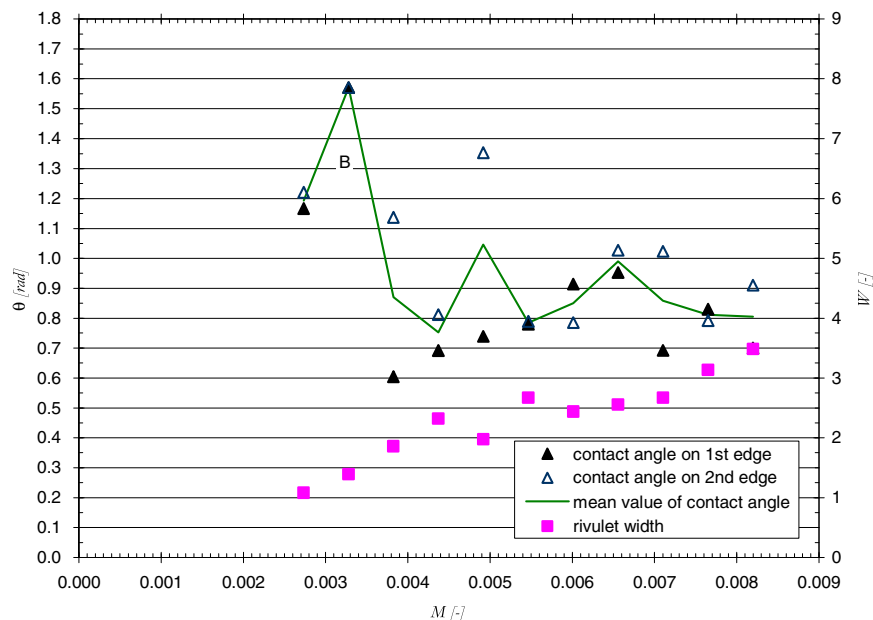


Fig. 12. Advancing contact angle on both edges and width of the rivulet on copper with roughness $R_a = 0.38 \mu\text{m}$.

The stage ends with the lowest value of the contact angle among the investigated metals and the median value of the width of the rivulet. In the third phase ($M > 0.006495$) the width and the contact angle increase simultaneously except the last point, where the contact angle slightly falls. Finally, the rivulet is the widest and the contact angle is the smallest of these metals.

2.3.2. The decrease of the flow rate

The disparities between the retreating contact angles on both edges are much smaller than between the advancing ones. The narrowing of rivulets on aluminium and brass are similar to each other and they are both completely different from that on copper.

When the mass flow is decreased the rivulet on copper narrows almost simultaneously but on the other metals the width of the rivulet remains constant (cf. Figs. 13, 16 and 19). Despite the fact that the rivulet on brass became narrower for the smaller mass flow rate than on aluminium, at the end of this stage the rivulet on the aluminium plate is wider than on the brass one.

The process on copper undergoes rapid changes. There is no correlation between the changes of the contact angle and the width, e.g., the contact angle and width may simultaneously decrease. It is expected, if the width becomes significantly smaller, that the contact angle will be constant or higher. This behaviour indicates that either the process is unstable or it is a neutral equilibrium.

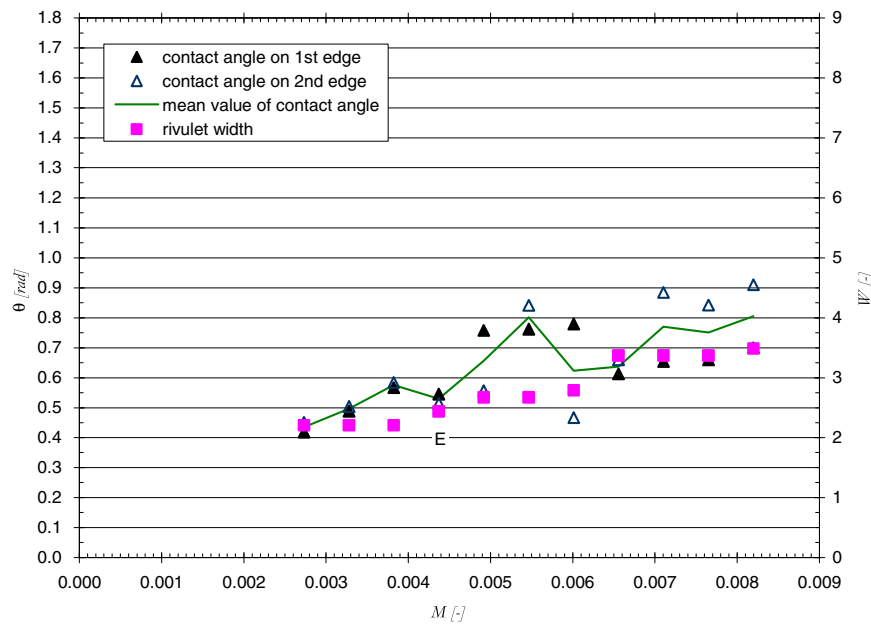


Fig. 13. Retreating contact angle on both edges and width of the rivulet on copper with roughness $R_a = 0.38 \mu\text{m}$.

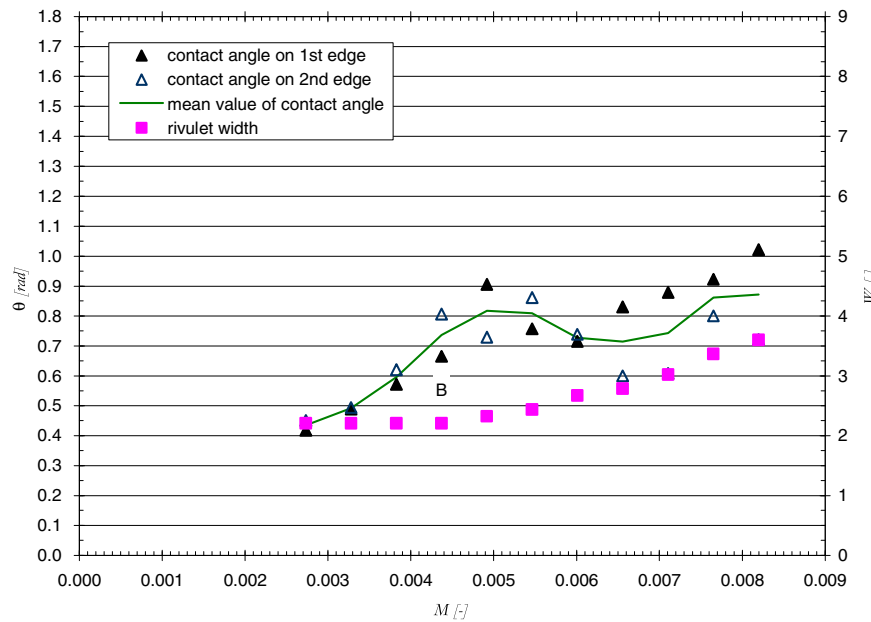


Fig. 14. Advancing contact angle on both edges and width of the rivulet on copper with roughness $R_a = 0.38 \mu\text{m}$, when the flow rate was increased again.

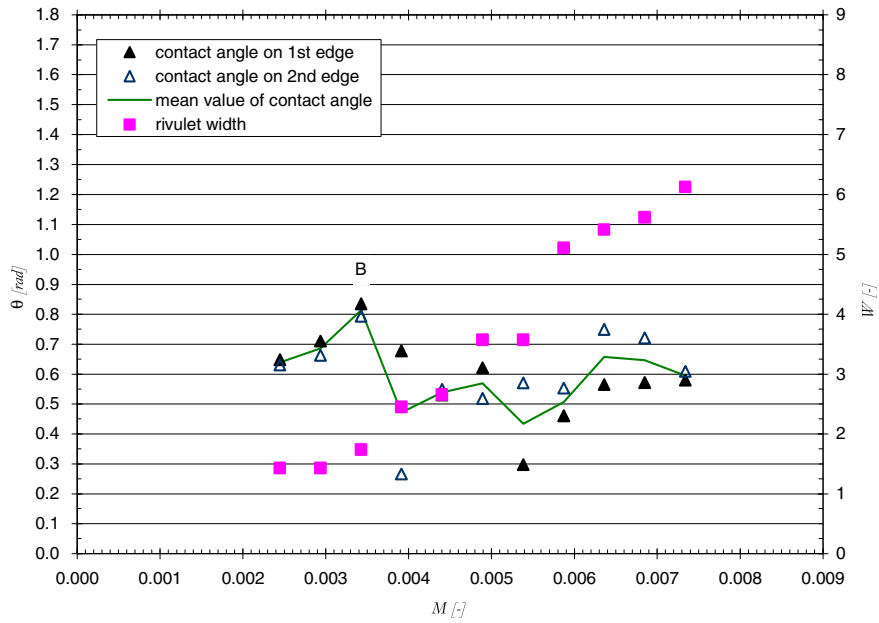


Fig. 15. Advancing contact angle on both edges and width of the rivulet on brass with roughness $R_a = 1.6 \mu\text{m}$.

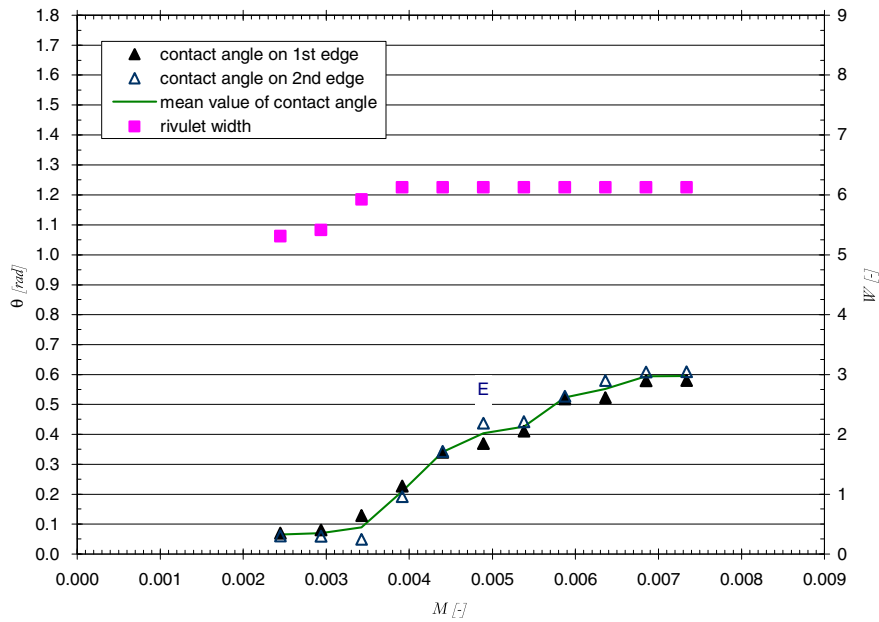


Fig. 16. Retreating contact angle on both edges and width of the rivulet on brass with roughness $R_a = 1.6 \mu\text{m}$.

The values of the contact angle are much higher and the width is much narrower than on aluminium or brass.

On brass in the first phase (for $0.00734 > M > 0.00391$) the width remains constant and the contact angle becomes smaller, although, at the beginning the contact angle slightly decreases. In the second phase (for $M < 0.00391$) the contact angle and the rivulet width decrease simultaneously.

On aluminium in the first phase (for $0.00812 > M > 0.00433$), the width is constant and the contact angle falls. The decreasing of the contact angle is much higher than on brass. In the second stage (for $M < 0.00433$) the width decreases and the contact angle remains almost constant.

Aluminium has the best hydrophilic properties, followed by brass. In spite of the fact that the contact angle values are smaller

than $\pi/2$, the behaviour of water on copper is similar to that on a hydrophobic surface.

2.3.3. The repeated increase of the flow rate

The rivulet widening on a previously wetted surface can be divided into two phases. In the first one the rivulet width is constant and the contact angle increases for each of the investigated metals. In the second stage the rivulet widens but the contact angle changes are different for each material. The final width on the metals is almost the same as in the initial stage of flow increase. On the copper plate the first phase ends for $M = 0.00437$. In the second phase the contact angle increases and decreases by turns. In the case of brass the first stage ends for $M = 0.00489$. The contact angle rises and at the end it decreases. The first phase is the longest on

aluminium and it ends for $M = 0.00704$ (see Fig. 20). In the second phase the contact angle increases and its value is almost equal to that on brass.

2.3.4. The comparison

The behaviour of water on a metal surface differs between static and flow conditions. In the first situation copper is a hydrophilic material, while brass and aluminium are hydrophobic. A disparate situation is observed when water flows: aluminium and brass lose their hydrophobic properties and become more hydrophilic than copper. The contact angle on copper is the highest of the investigated metals (there are only two points in the graph for aluminium and one for brass with higher mean contact angle values for the same flow rate, e.g., for $M \cong 0.00435$ and

$M \cong 0.0054$ in Figs. 12 and 18) as well as for $M \cong 0.0064$ in Figs. 14 and 17. The rivulet on copper is narrower than on brass at every point and on aluminium for $M > 0.00595$. At the first point the rivulet width on copper equals that on aluminium, while on brass it is wider. The widening on copper and brass to $M \cong 0.00437$ has the same inclination to the M -axis, but on aluminium to $M \cong 0.00487$ the rivulet has almost the same width. For the higher mass flow rates, the rivulet on copper widens more slowly, but on aluminium the average growth in width is the biggest. At the end, the rivulet on aluminium is the widest of the investigated metals. In contrast, under static conditions [12] no impact of drop volume on the improvement or deterioration in the wetting properties of a metal in relation to the others was observed.

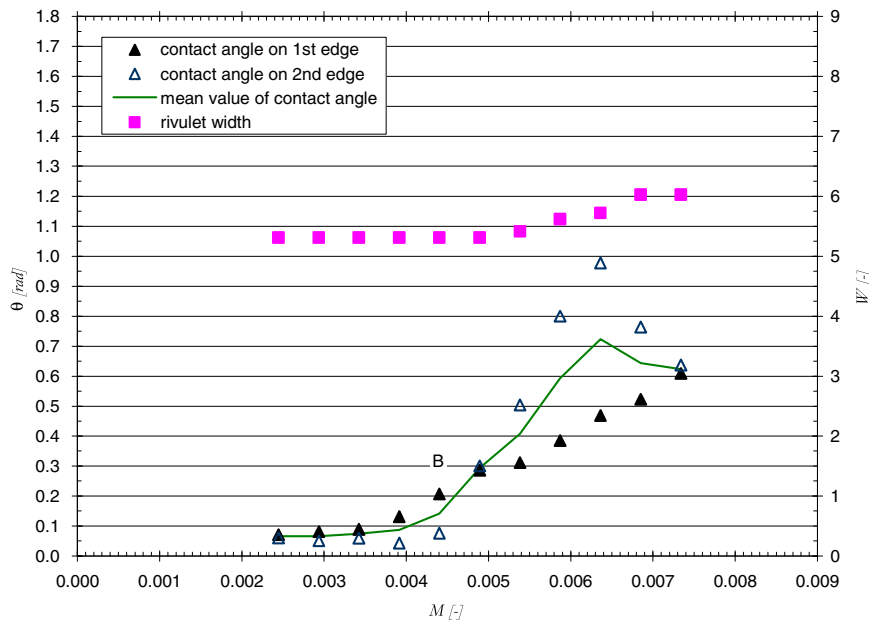


Fig. 17. Advancing contact angle on both edges and width of the rivulet on brass with roughness $R_a = 1.6 \mu\text{m}$, when the flow rate was increased again.

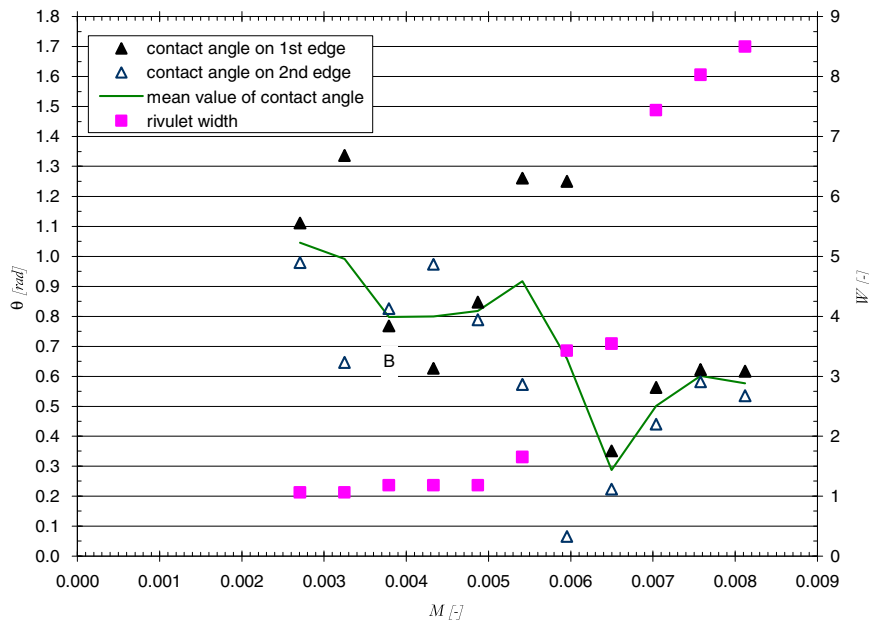


Fig. 18. Advancing contact angle on both edges and width of the rivulet on aluminium with roughness $R_a = 1.38 \mu\text{m}$.

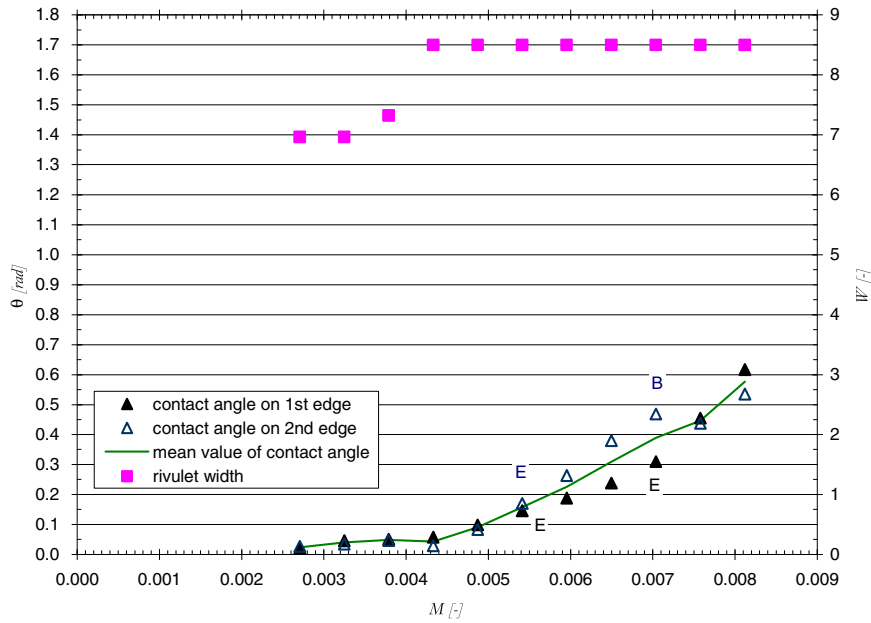


Fig. 19. Retreating contact angle on both edges and width of the rivulet on aluminium with roughness $R_a = 1.38 \mu\text{m}$.

The latter observations suggest that the mass flow rate of water influences the chemical properties of metals. The surfaces of the aluminium and brass plates have been covered with a thin layer of oxide for several years, and small black rings of copper oxide are scattered on the plate. The zinc (brass consists of copper and zinc) and aluminium oxides are hydrophobic, so it is expected that brass and aluminium should have the worst wetting properties. However copper, which is not covered by a continuous oxide layer, should have the best wetting properties. Such a situation was observed in the static conditions, see [12] and [6]. The investigations of Kim et al. [9] cast light on the strange metal behaviour. They discovered that the barrier layer in the porous oxide films on aluminium dissolves electrochemically. The process is assisted by an electrical field across the barrier layer – solution interface. It is

interesting to note that even “pure water” at pH 7 is an electrolyte solution with 10^{-7} mol/dm^3 of H_3O^+ and the same amount of OH^- ions. It can be assumed that the moving ions create an electrical field, the faster they move, the higher current flows. This might explain the rapid increase of the rivulet width on aluminium. The alloy of copper and zinc is covered by an oxide film similarly to aluminium, but the rivulet on brass is wider than on copper even at the starting point. The dissolution of the oxide film on brass might have started much earlier than in the case of aluminium. It seems that the flow of hydroniums and hydroxides between Cu^+ and Zn^{2+} ions creates an electrical field, which speeds up the dissolution of the oxide film.

For $M > 0.00685$, when the oxide barriers on aluminium and zinc seem to be removed completely, the best wetting properties

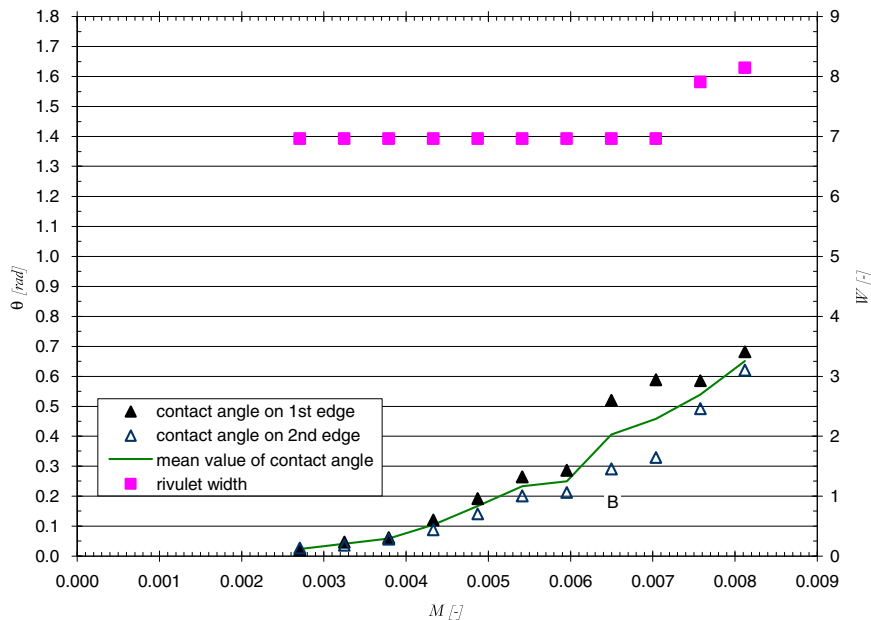


Fig. 20. Advancing contact angle on both edges and width of the rivulet on aluminium with roughness $R_a = 1.38 \mu\text{m}$, when the flow rate was increased again.

has aluminium, followed by brass and copper. Such order might be caused by the quantity of electrons on the last electron shell. The more electrons there are the stronger attractive forces interact between metal and water. An atom of aluminium has 3 electrons on the M shell, an atom of zinc has 2 electrons on the N shell, and an atom of copper has 1 electron on the N shell.

3. Conclusions

The comparison between experiments under flow conditions and static conditions leads to the following conclusions:

1. The wetting properties of a dipole liquid on a metal surface are different under flow conditions and static conditions.
2. The wetting properties examined for sessile drops cannot be extrapolated to rivulets.
3. The contact angle should be measured on both edges of the rivulet.
4. The more electrons there are on the last metal shell, the more hydrophilic properties a metal has under flow conditions.

Acknowledgement

The scientific work was funded by a grant from The State Committee for Scientific Research between 2003 and 2006.

References

- [1] T. Hobler, Minimum surface wetting (in Polish), *Chemia stosowana* 2B (1964) 145–159.
- [2] I. Langmuir, V.J. Schaefer, The effect of dissolved salts on insoluble monolayers, *I.J. Am. Chem. Soc.* 59 (1937) 2405.
- [3] G.D. Towell, L.B. Rothfeld, Hydrodynamics of rivulet flow, *A.I.Ch.E. J.* 12 (5) (1966) 972–980.
- [4] S. Semiczek-Szulc, J. Mikielewicz, Experimental investigations of contact angles of rivulets flowing down a vertical solid surface, *Intl. J. Heat Mass Trans.* 21 (1978) 1625.
- [5] S. Hirasawa, E.G. Hauptmann, Dynamic contact angle of a rivulet flowing down a vertical heated wall, 8th International Heat Transfer Conference, vol. 4, San Francisco, CA, USA, 1986, pp. 17–22.
- [6] R. Rybnik, M. Trela, Influence of substrate material and surface roughness on the contact angle of sessile drops, *Wärmeaustausch und Erneuerbare Energiequellen, VII Internationales Symposium Szczecin-Swinoujście 7–9.09.1998, Tagungsmaterialien*, 315–322.
- [7] A. Marmur, Contact angle hysteresis on heterogeneous smooth surface, *J. Colloid Interface Sci.* 168 (1994) 40–46.
- [8] A. Marmur, Simulated contact angle hysteresis of a three-dimensional drop on a chemically heterogeneous surface: a numerical example, *Adv. Colloid Interface Sci.* 50 (1994) 121.
- [9] Y.-S. Kim, S.-I. Pyun, S.-M. Moon, J.-D. Kim, The effect of applied potential and pH on the electrochemical dissolution of barrier layer in porous anodic oxide film on pure aluminium, *Corrosion Sci.* 38 (2) (1996) 329–336.
- [10] A. Gajewski, M. Trela, Effect of rivulet mass flow rate on the surface wetted area, *Arch. Thermodyn.* 23 (1–2) (2002) 101–125.
- [11] A. Gajewski, A method for contact angle measurements under flow conditions, *Intl. J. Heat Mass Trans.* 48 (2005) 4829–4834.
- [12] A. Gajewski, Contact angle and sessile drop diameter hysteresis on metal surfaces, *Intl. J. Heat Mass Trans.* (2008), doi:10.1016/j.ijheatmasstransfer.2008.01.027.